

## Acoustic Borehole Televiwer Results from CRP-2/2A, Victoria Land Basin, Antarctica

D. MOOS<sup>1\*</sup>, R. D. JARRARD<sup>2</sup>, T. S. PAULSEN<sup>3,4</sup>, E. SCHOLZ<sup>5</sup> & T.J. WILSON<sup>3</sup>

<sup>1</sup>Department of Geophysics Stanford University, Stanford, CA 94305-2215 - USA

(present address: GeoMechanics International, Inc. 250 Cambridge Ave., Suite 103, Palo Alto, CA 94306 - USA)

<sup>2</sup>Department of Geology and Geophysics, Univ. of Utah, 135 S. 1460 East, Rm 719, Salt Lake City, UT 84112 - USA

<sup>3</sup>Byrd Polar Research Center and Dept. of Geological Sciences, Ohio State University 1090 Carmack Rd., Columbus, OH 43210 - USA

<sup>4</sup>Department of Geology, University of Wisconsin-Oshkosh 800 Algoma Blvd., Oshkosh, WI 54901 - USA

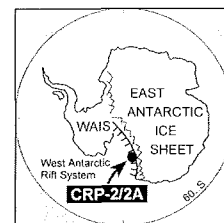
<sup>5</sup>Lamont-Doherty Earth Observatory, Palisades, NY 10964 - USA<sup>4</sup>

\*Corresponding author (moos@geomi.com)

Received 13 August 1999; accepted in revised form 19 June 2000

**Abstract** - Acoustic borehole televiwer (BHTV) data were recorded in both the HQ (64 to 164 m below sea floor) and the NQ (196 to 444 mbsf) sections of the CRP-2 borehole. The purpose of logging this hole with the BHTV was to provide images of the borehole wall to detect and orient natural fractures, stratigraphy, and stress-induced features (breakouts and tensile fractures). It was also hoped that the BHTV data could be used to orient the cores, provided it was possible to identify the same features in both data. The upper log was recorded without orientation, whereas the lower log was oriented with respect to the earth's magnetic field using a single-axis magnetometer. The results revealed stratigraphic and structural features of the rock penetrated by the borehole. In general, stratigraphic boundaries dip gently east-northeast, as also revealed by analysis of a dipmeter log (Jarrard et al., this volume). Fractures have steep, generally west, dips. No stress-induced wellbore breakouts were detected in this hole. However, numerous subvertical fractures were observed coinciding with "core-edge fractures" identified in the core. In the lower logged interval these fractures had a consistent N10W/S10E strike. Although the core-edge fractures appear to be concentrated on only one side of the borehole, some features appear on both sides of the hole, and therefore core orientations, where these could not be associated with individual features in the BHTV data, have a +/- 180 degree ambiguity. These features may be useful to orient both the un-oriented BHTV data in the upper section and the core with the same ambiguity.

The stress state which best explains the orientation and occurrence of the core-edge fractures and the absence of breakouts is one in which  $SH_{min} < SH_{max} \leq Sv$ , and  $SH_{max}$  is oriented N10W/S10E. This stress orientation and the normal to strike-slip stress magnitude is consistent with pure normal faulting along the local trend of the Transantarctic Mountains.



### INTRODUCTION AND PURPOSE OF MEASUREMENTS

The Cape Roberts Project (CRP) is an international drilling program whose aim is to reconstruct Neogene to Paleogene paleoclimate and tectonic history, by continuous coring and well logging at sites near Cape Roberts, Antarctica. The first CRP drillhole, CRP-1, obtained 148 meters of Quaternary and Miocene sediments (CRST, 1998). The second CRP drillhole, CRP-2, extended to 625 meters below sea floor with an average 95% recovery of Oligocene to Quaternary sediments (CRST, 1999).

BHTV data were acquired in CRP-2 primarily to identify and characterize stress-induced breakouts and other drilling-induced failures. The orientation and characteristics of drilling-induced failures provide considerable information about the orientation and magnitudes of the *in situ* tectonic stresses. In addition, the BHTV images were analyzed to detect, delineate and orient natural fractures and stratigraphic features. Finally, it was hoped that the BHTV data would provide information to orient the core recovered during

drilling based on correlation of geological and drilling-induced features seen in both BHTV images and in the core (Paulsen et al., this volume). Additional logs, including geophysical logs of rock properties and dipmeter logs to determine stratigraphic and structural orientations, were also acquired in the borehole. The analysis and interpretation of these logs are described in Brink & Jarrard (this volume), Brink et al. (this volume), Bucker et al. (this volume) and Jarrard et al. (this volume).

Wellbore failures controlled by the *in situ* tectonic stress form the basis for most of the stress orientations catalogued in the World Stress Map (*e.g.*, Zoback, et al., 1989). However, because of the lack of drilling within the Antarctic plate and the relative paucity of any other commonly used stress indicators, little information exists to characterize the plate-wide stress state within Antarctica. In the region of the Cape Roberts drill site, knowledge of the present-day state of stress is crucial to resolve ambiguities concerning the formation and continued deformation of the Transantarctic Mountains - Victoria Land rift basin structural boundary.

## THE BHTV LOG

The BHTV (borehole televiewer) is an acoustic device which provides an image of the surface (acoustic) reflectivity of the wall of a fluid-filled hole, as first described by Zemanek et al. (1970). As the tool is pulled up the hole, pulses fired in rapid sequence from an acoustic transducer mounted on a rotating shaft are reflected from the wall of the hole and returned to the transducer. The amplitude of the returned pulse is primarily a function of the acoustic reflectivity and roughness of the wall of the hole. The time of flight can be used to compute the radius of the hole along the trajectory traversed by each reflected signal. The reflection point follows a helical trajectory along the wall. The data are oriented magnetically using a single-axis magnetometer mounted on the rotating shaft, to allow an oriented image to be formed of the amplitude of the reflected signal and of the computed borehole radius. An example of data from CRP-2 is provided in figure 1 and is discussed in more detail below.

The BHTV can be used to detect variations in surface roughness of the borehole wall associated with stratigraphic changes, thereby making it possible to carry out detailed stratigraphic analyses. Where contacts and internal structures have sufficient dip, it is possible also to orient these features. Non-planar features and contacts can also be detected and analyzed. Using the orientations of these features and relating them to the same features in the core provides a means of core orientation, as long as the features can be observed in both data sets.

The process of drilling a borehole may induce wellbore breakouts (compressive failures which cause wellbore enlargements at the orientation of the least horizontal tectonic stress) and tensile wall cracks (tensile failures which occur at the orientation of the greatest horizontal principal stress). Detection of these features in vertical holes allows determination of the orientation of the *in situ* horizontal stresses. Their presence or absence provides quantitative information about the horizontal stress magnitudes.

In some cases coring induced failures, caused by the stress concentration below the bit, are formed prior to cutting the core. These coring induced failures can often be identified in the recovered core. Where these extend along the walls of the hole they can also be detected in BHTV data.

## FIELD ACTIVITIES AND DATA PROCESSING

BHTV data were acquired during two phases of drilling of CRP-2. The first phase occurred at the end of the initial drilling of HQ hole. During this logging run, which acquired data from 64 to 164 mbsf no orientations were acquired because of the necessity to overdrive the electronics to maintain transducer rotations in this cold environment. This log was extended into casing to provide a tie point for depth against driller's depths. During Phase 2 of logging, the NQ hole was logged with magnetic orientation from slightly above the bottom of casing 196 mbsf to a bridge encountered at 444 mbsf. The deepest

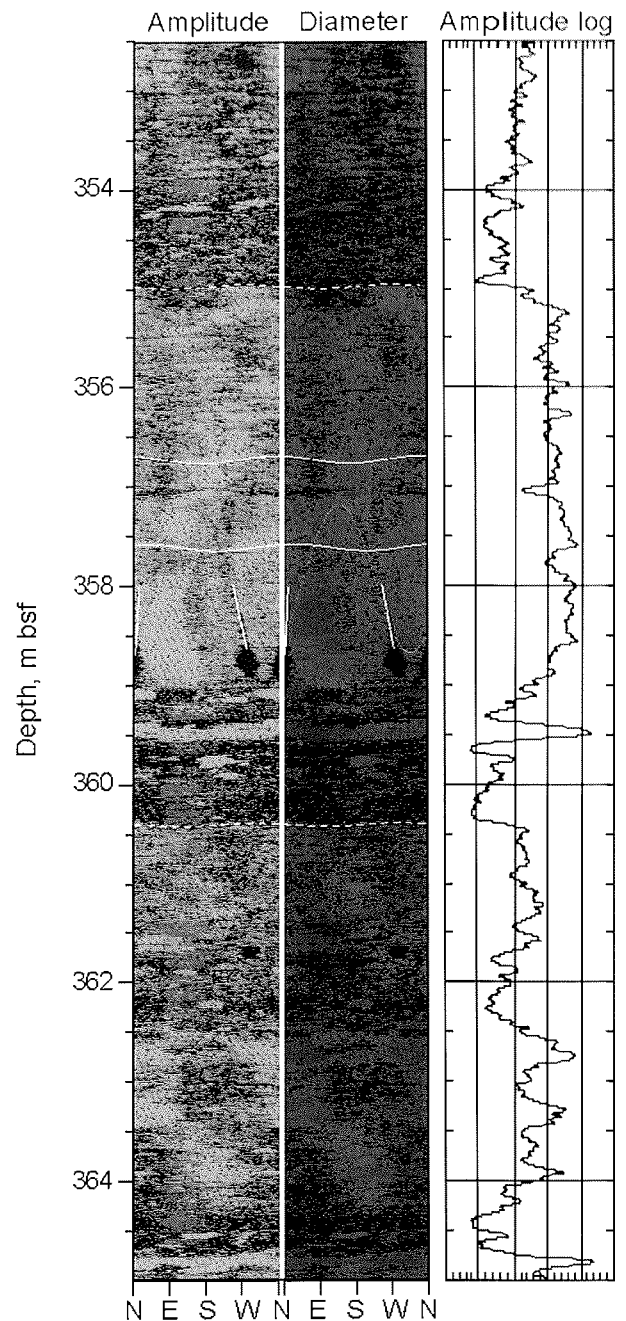


Fig. 1 - BHTV images of amplitude and hole radius, acquired over the interval 352.5 to 365 m in CRP-2. The images display unwrapped views of the properties of the borehole, cut at geographic north and laid flat. Also shown is a mean amplitude log computed from the image data.

181 m of hole below this depth could not be logged due to the presence of the bridge. During logging polaroid pictures were taken of the amplitude image of the borehole. Analog data were written to videotape for later digitization, enhancement, and extraction of time-of-flight data to compute hole radius.

Considerable concern was expressed about the ability of the single-axis magnetometer within the tool to provide a reliable orientation for the images because of the steep inclination of the magnetic field vector at the site. This proved not to be a problem during Phase 2 of logging. However, until Phase 2 data was acquired with magnetic orientation this was assumed to be the explanation for the

inability to orient the tool magnetically during Phase 1. A more serious problem was the potentially large variation in magnetic declination associated with magnetic storms. The careful process outlined in Jarrard et al. (this volume) that was employed to identify and correct for such variations in the dipmeter data was not carried out during acquisition of the BHTV data. The consistency of orientation with depth of coring-induced features in the BHTV images discussed below provides considerable confidence that magnetic storms did not affect declination during this log. We use the same fixed value of declination of 148 degrees that was used by Jarrard et al. to correct from magnetic to geographic orientation of the images from Phase 2 of logging.

After completion of field activities, the analog data recorded on videotape was digitized to allow interactive analysis using computer software (Barton et al., 1988). Data were carefully quality-controlled using the polaroid pictures for reference. Travel-times were converted to radius using the known radius of casing and a value for the acoustic velocity of sound in the borehole fluid of 1524 m/s. A correction from measured depth to depth below sea floor was made by subtracting 180.2 meters from the depths recorded during logging. The resulting depths were verified using features that could be clearly seen in both core and BHTV data. The depths of these features are known to within 0.5 meters. After these corrections were applied, the data were analyzed to determine the orientations and depths of natural and drilling-induced fractures and stratigraphy.

Figure 1 shows a section of BHTV data recorded during Phase 2 of logging over the interval 352.5 to 365 mbsf. The reflected amplitude image is shown as a function of depth and azimuth in the left-hand track. Lighter values correspond to higher reflected amplitudes. In the center is the radius image of the borehole. Darker values are closer to the tool, indicating a smaller radius. On the right is shown an amplitude log derived from the amplitude image. Superimposed on the image are symbols indicating natural and drilling-induced features picked interactively from the images. The results of analysis of all of the features revealed by the BHTV images are discussed below.

The near-vertical light-colored bars in figure 1 identify a set of coring-induced fractures. The fractures picked here at 358 m depth occur as a pair of near-vertical features that get closer together with increasing depth. They cut a chord across the borehole. At the base of these fractures is a small "trough" that is the exit point of the fracture from the borehole. There is no evidence that these fractures cross the hole – they simply stop at some uphole point. These features are characteristic of the "core-edge fractures" that are discussed in Paulsen et al. (this volume).

Natural fractures are picked interactively using a flexible sinusoid (Barton et al., 1988). Light-colored, solid sinusoidal traces identify the picked fractures in figure 1. Light-colored, dashed sinusoidal traces identify planar features that appear to be stratigraphic boundaries, because they often separate rock with different acoustic characteristics (principally reflected amplitude). By averaging the reflected amplitude across the hole at each

depth, an amplitude log can be prepared which reveals very fine-scale stratigraphic units, as shown in figure 1 (for example, the ~20-cm-thick highly reflective interval at 359.5 m). Because limestones are often more reflective than the surrounding material, they may also be detected using average reflected amplitude.

## NATURAL FEATURES

Planar features that cross the borehole appear as sinusoidal traces on the BHTV image. The feature dip can be computed as the inverse tangent of the ratio of the height of the sinusoid to the diameter of the borehole at the feature depth ( $\text{dip} = \tan^{-1}(h/d)$ ). Both of these parameters can be measured from the BHTV data. The dip direction is the orientation of the trough of the sinusoid. It is not always possible to differentiate between stratigraphic boundaries and fractures. In some cases the distinction is quite clear because, in general, a stratigraphic boundary juxtaposes material with very different acoustic characteristics, whereas a fracture can be contained within a single unit or can cross a unit boundary. In other cases it is not so clear, and in the CRP-2 borehole it was often difficult to classify features using only their characteristics observed in the images.

Because its vertical resolution is limited by the finite logging rate and the small diameter of the CRP-2 borehole, features in the BHTV images with dips less than 6 degrees (in Phase 1) and 8 degrees (in Phase 2) could not be oriented. Furthermore, the orientations of features with dips less than 12 and 15 degrees, respectively, have large uncertainties. Features that dip more than 45 degrees can be very accurately oriented.

## FRACTURES

Fractures can be seen by the BHTV because the reflected amplitude is reduced when the signal encounters the increased borehole wall roughness adjacent to the fracture that often occurs during drilling. Because some fractures do not erode sufficiently during drilling, not all fractures are detected. Furthermore, the apparent aperture of a fracture on the image is a consequence of drilling-induced damage in addition to its properties away from the well.

Numerous fractures were detected in the images from both phases of BHTV logging in CRP-2. Plots of fracture dips and dip directions are presented in figure 2. Figure 3 presents lower hemisphere stereographic projections of poles to the fractures whose dip direction could be determined. In general, fractures observed in both phases of logging dip steeply (60 to 80 degrees) and in Phase 2 have dip directions to the east and west. The steepest fractures dip to the west south-west. A significant subset of fractures have shallower dips, however. These shallow dips are present throughout the depth range and may be stratigraphic in origin. Either they are bedding planes or they are fractures initiated along the bedding planes. Fewer fractures were observed in softer rocks where reflected amplitudes were lower, and while this may

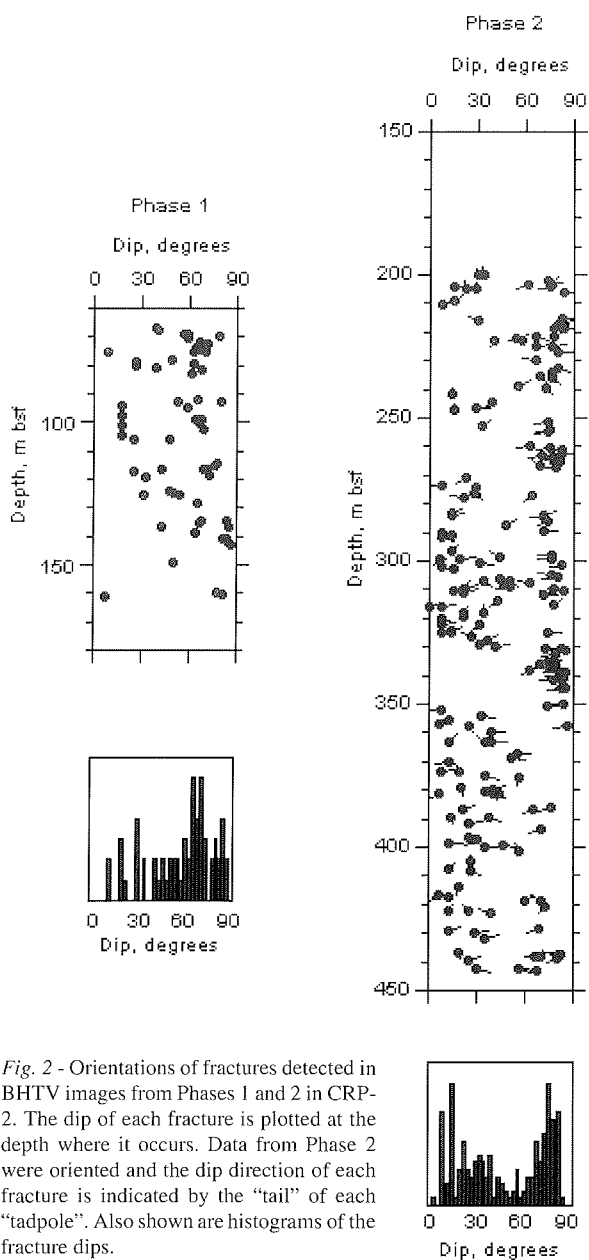


Fig. 2 - Orientations of fractures detected in BHTV images from Phases 1 and 2 in CRP-2. The dip of each fracture is plotted at the depth where it occurs. Data from Phase 2 were oriented and the dip direction of each fracture is indicated by the "tail" of each "tadpole". Also shown are histograms of the fracture dips.

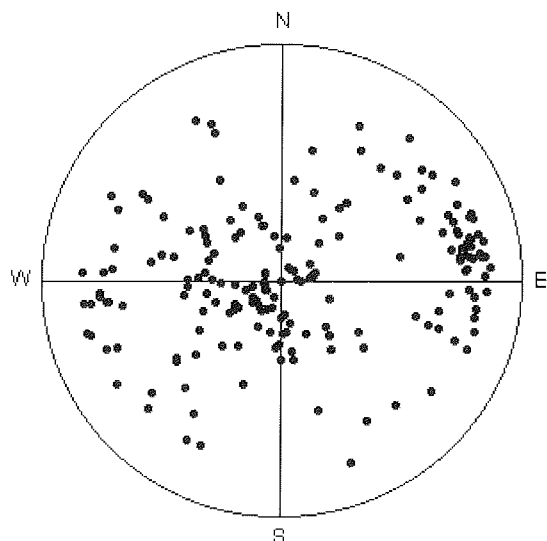


Fig. 3 - Stereographic lower hemisphere projection of directions normal to fractures detected in BHTV image data from Phase 2.

indicate that these units are less fractured it may be simply that fractures were easier to detect in more competent highly reflective units.

Core analyses detected many more fractures than were detected in the BHTV images. Where fractures detected by the BHTV could be correlated to fractures measured in cores, it is possible to use the BHTV to orient the core (Paulsen et al., this volume). The best orientations came from correlating the induced fractures, however, as it was easier to relate specific induced fractures within the core and borehole images than it was to relate individual natural fractures.

### STRATIGRAPHY

The BHTV can be used to detect variations in reflectivity of the borehole wall by computing the mean reflectivity at each depth and presenting the results as a log. If the wall were perfectly smooth and the BHTV were perfectly centered, then the only variation in amplitude would be associated with changes in the acoustic impedance (density times velocity) of the wall of the hole. However, wellbore roughness, hole size changes, intersecting fractures and other damage to the hole wall also contribute to the signal. In spite of this, relative amplitude logs can be used to identify stratigraphic variations along the borehole (see Fig. 1).

Figure 4 shows relative amplitude as a function of depth for Phases 1 and 2. Amplitudes cannot be compared between the two Phases, as hole size, tool and digitization parameters were different between the two runs. Within each run, however, tool and digitization parameters were kept constant. Significant variations in reflected amplitudes can be seen in both sets of data. There is in many places a remarkable correlation between relative amplitude and geophysical logs such as susceptibility (the logs and the log analysis are described in Wonik et al., this volume).

The BHTV data were also analyzed to identify and orient individual stratigraphic boundaries and to detect internal stratigraphic features. The results are plotted as a function of depth in figure 5. Figure 6 shows a lower hemisphere stereographic projection of the poles to the stratigraphic planes. In general, boundaries have quite shallow dips (below 30 degrees) and thus the orientations of these features are not very precise. Where dip directions could be determined, stratigraphic features primarily dip to the east. There are also a number of shallow, west dipping, features, and some contacts appear to be steeply dipping. As shown in figure 1, however, not all contacts are planar. Such non-planar contacts and anomalous steep dips may be associated with drape on limestones, or may be due to soft-sediment deformation, as also suggested by Jarrard et al. (this volume).

### DRILLING INDUCED FEATURES

The process of drilling a borehole causes a concentration of stresses around the borehole wall (Kirsch, 1898; Zoback et al.; 1985, among others) and below the bit (Li and

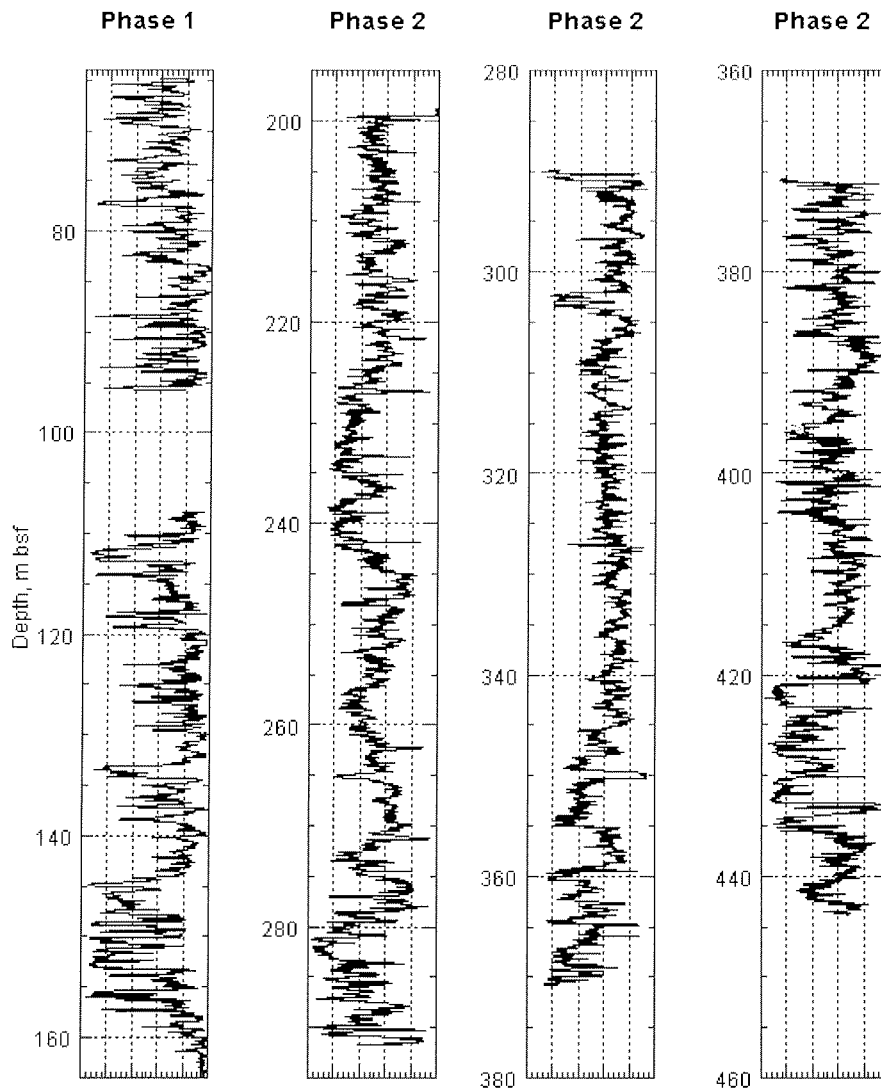


Fig. 4 - Amplitude logs computed from BHTV images of CRP-2.

Schmitt, 1997). Where the compressive stress concentration around the wall of the hole is larger than the rock strength, the rock fails and falls into the hole, forming a borehole breakout (Gough and Bell, 1981). Breakouts form on opposite sides of a hole and can be detected with 4-arm caliper logs, if they are large enough, and with imaging tools like the BHTV, even when they are too small to be detected by caliper logs. In vertical holes, breakouts occur at the azimuth of the least horizontal far-field stress and can be used to determine the *in situ* orientations of the maximum and minimum horizontal stresses. The occurrence (or non-occurrence) of breakouts and their widths can be used to quantify stress magnitudes (Zoback et al., 1985; Moos and Zoback, 1990).

Drilling-induced tensile wall fractures can form at the wall of a vertical borehole if the horizontal stress difference is very large, due to the tensile stress that forms at the azimuth of the far-field greatest horizontal stress. In wells which are drilled with a mud weight only slightly greater than the pore pressure (as was the case for CRP-2), their presence requires a very large difference in horizontal stresses.

The large stress concentration induced below the coring bit can also lead to tensile fractures that form below the bottom of the hole. At depth, these often form near the hole center, and are thus often referred to as petal center-line fractures (e.g., Lorenz et al., 1990). In other cases these can form at the edges of the borehole ("core-edge" fractures). Coring-induced fractures have quite characteristic features, as discussed in more detail by Paulsen et al. (this volume). They can be differentiated from natural fractures because they do not cross the well and thus do not form complete sinusoids.

Numerous "core edge" fractures were detected in cores from CRP-2 (Paulsen, this volume). As in the case of tensile wall fractures, the presence of these features is an indication of a large difference in horizontal stresses. Furthermore, it is likely that their occurrence at the edges of the borehole, rather than through its center, is a consequence of the relatively shallow depths penetrated by CRP-2 (Li and Schmitt; 1997; 1998). Regardless of whether these features occur through the center or along the edge of the core, they strike in the direction of the far-field greatest horizontal stress.

**DRILLING-INDUCED FEATURES  
IN BHTV IMAGES**

**CORE-EDGE FRACTURES**

Figure 1 shows an example of a drilling-induced “core-edge” fracture at a depth of 358 m bsf. The exit point at the base of the feature is quite clear, as are the limbs that extend downward to that point. In order to determine the orientation of these features, the orientation of each limb was first determined as shown in the figure. The strike of each feature was then computed as 90 degrees plus the average of the limb orientations.

The depths and apparent orientations of all of these features are presented in figures 7 and 8, for Phases 1 and 2, respectively, of BHTV logging of CRP-2. Phase 1 orientations are relative as the BHTV data were not oriented during this log; the purpose of presenting these data is to indicate the depths at which these features were identified.

Drilling-induced fractures occur throughout the logged depth. They concentrate (particularly in the Phase 2 data) within units with higher reflected amplitudes. This is most likely because it is easier to detect fractures in those units, but it may also be related to the rock properties—units with higher reflected amplitudes may be stiffer and more brittle and thus more prone to tensile failure.

In Phase 2 there is a strong preferred orientation of these features slightly to the east of south (170 degrees). There are very few features with other orientations. It is interesting also that there are relatively fewer features with computed orientations of N10W. This reveals that these features tend to form closer to the east side of the borehole and occur less often on the western side. If the eastern orientation is more common, it could either be a consequence of an asymmetry in the rock fabric (for example, a consistent east dip) or in the hole orientation with respect to the principal stresses. For example, a slight inclination of the principal stress axes to the east or west, or a slight hole deviation, could generate an asymmetry of this sort. The preferred orientation of these coring-induced features may help to remove a +/- 180 degree ambiguity in their orientation and allow core orientation even when a core-edge fracture could not be associated with a feature observed in the BHTV images.

**BREAKOUTS AND TENSILE WALL CRACKS**

No breakouts were detected in BHTV logs of the CRP-2 borehole. This confirms the results of Montoué et al., who also saw no evidence of wellbore breakouts. However, in addition to the core-edge fractures identified in the BHTV logs, there are indications of a few tensile wall fractures that occur 180 degrees apart on opposite sides of the hole. Their orientations are consistent with those of the core-edge fractures and require an N10W/S10E orientation of maximum horizontal stress. The presence of these features requires a large difference in horizontal stresses. The absence of breakouts places an upper bound on the magnitudes of the horizontal stresses. Taken together, these data provide a means to define the stress state within the interval cored by CRP-2.

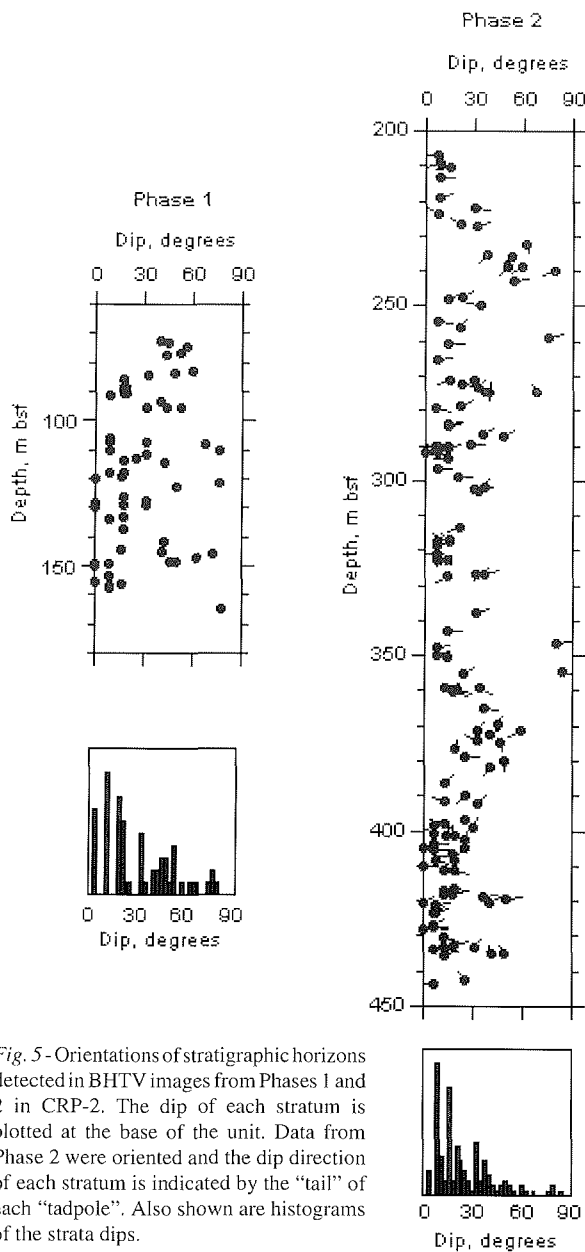


Fig. 5- Orientations of stratigraphic horizons detected in BHTV images from Phases 1 and 2 in CRP-2. The dip of each stratum is plotted at the base of the unit. Data from Phase 2 were oriented and the dip direction of each stratum is indicated by the “tail” of each “tadpole”. Also shown are histograms of the strata dips.

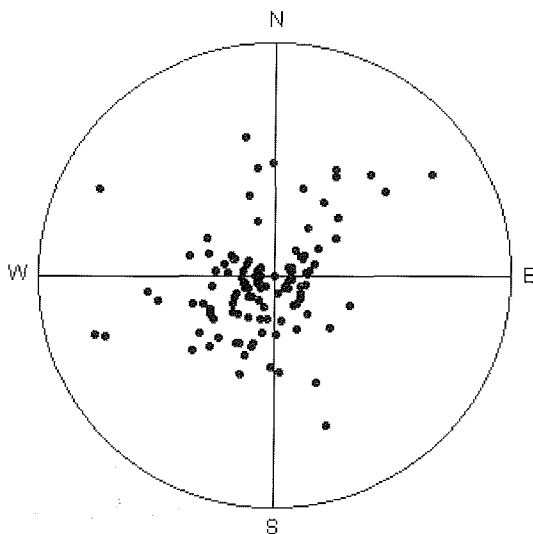


Fig. 6- Stereographic lower hemisphere projection of directions normal to stratigraphic horizons detected in BHTV image data from Phase 2.

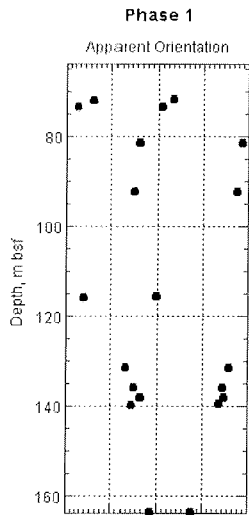


Fig. 7 - Positions (depth and apparent orientations) of tensile (core-edge) fractures detected in BHTV images acquired during Phase 1. The orientations are not reliable, but the depths are accurate and can be used to compare these features with similar features on the core.

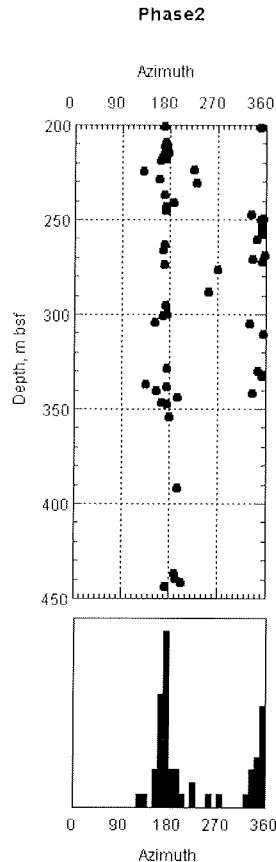


Fig. 8 - Positions (depth and geographical orientations) of tensile (core-edge) fractures detected in BHTV images acquired during Phase 2. Also shown is a histogram of the azimuths of the tensile fractures detected in Phase 2 images.

## IMPLICATIONS FOR STRESS ORIENTATION AND MAGNITUDE

Based on the mean orientation of the core-edge fractures and of the few tensile cracks that appear in the oriented BHTV images, the azimuth of the greatest horizontal stress is N10W/S10E within the interval cored by CRP-2 (Fig. 8).

Furthermore, the presence of tensile features and the absence of compressive features together provides information to constrain the magnitudes of the horizontal stresses. This process requires knowledge of the mud weight used to drill the hole and the maximum surface pumping pressure (8.8 lbs/gal and 225-400 psi; written comm, 1999), and the hole orientation (within 1 degree of vertical; Jarrard et al., this volume). Thus the mud pressure acting against the walls of the hole while drilling was equal or slightly greater than the pore pressure. The hole was vertical. Equations 1 and 2 define the stresses necessary for tensile failures to occur without the occurrence of breakouts for these conditions. If the tensile strength ( $T$ ) and the unconfined compressive strength ( $UCS$ ) are known, these equations can be solved to constrain the stress magnitudes, where  $SH_{max}$  is the maximum horizontal

stress,  $Sh_{min}$  is the minimum horizontal stress,  $P_p$  is the *in situ* pore pressure, and  $P_m$  is the mud pressure. The fact that drilling-induced tensile wall cracks are aligned parallel to the borehole axis indicates that the well was drilled along a principal stress direction, and this means that the principal stresses act in vertical and horizontal directions (the principal stress axes are parallel and perpendicular to the earth's surface).

No compressive failure:

$$UCS \leq 3SH_{max} - Sh_{min} - 2P_p - (P_m - P_p) \quad \text{Eqn 1.}$$

Tensile failure:

$$SH_{max} \geq 3Sh_{min} - 2P_p + T - (P_m - P_p). \quad \text{Eqn 2.}$$

An additional method to constrain the *in situ* stresses is to rely on the additional observation that stress in the earth's crust is limited by the frictional strength of faults (Zoback and Healy, 1984). This constraint places an upper bound on the ratio of greatest to least effective principal stress, defined by  $(S_1 - P_p)/(S_3 - P_p) = f(\mu)$ , where  $\mu$  is the coefficient of sliding friction along the fault surface. Laboratory experiments demonstrate that  $\mu$  varies between 0.6 and 1.0 (Byerlee, 1978). Thus this equation provides a means to define the limits of the possible stress magnitudes at any depth, using the vertical stress computed from the weight of the overlying rock as a tie point.

Figure 9 shows the stress limits appropriate for a depth of 500 meters. A mean density of 2.2 is used for convenience, yielding a vertical stress at this depth of 11 MPa plus the weight of the water column, which adds an additional 1.8 MPa. There was some evidence of slight overpressure based on driller's reports, leading to a slight overpressure above hydrostatic ( $P_p = 6.8$  MPa). The effective mud pressure, using the mud weight of 8.8 lb/gal and the depth correction from rig floor to mud line of 180.2 m, is only slightly higher (7 MPa); dynamic effects while circulating add an additional pressure somewhat less than the surface pumping pressure, and so we assume 1 MPa overbalance.

Also shown in figure 9 are lines illustrating the values of the horizontal stress magnitudes required to form tensile fractures in the CRP-2 borehole. These lines approximately parallel the strike-slip faulting limit. Because the rock is extremely weak, the presence of tensile features requires that  $SH_{max}$  lie above the line corresponding to an effective tensile strength approximately equal to zero. Also shown are red lines that define the states above which breakouts would occur for the given UCS. If the UCS of these rocks were 10 MPa (based on the low velocities and densities measured in these rocks, some may have even lower strengths), the lack of breakouts requires that the stress state within the basin lie below the red line labeled 10 on the plot. The frictional limits require that the stresses lie inside the polygon. These considerations restrict the stress state to lie within the shaded region shown in Fig. 9. This is a normal to strike-slip faulting stress state. Further quantification of the stress state would require either measurements of UCS on samples from the borehole, or conducting an hydraulic fracturing experiment to directly measure the horizontal stresses.

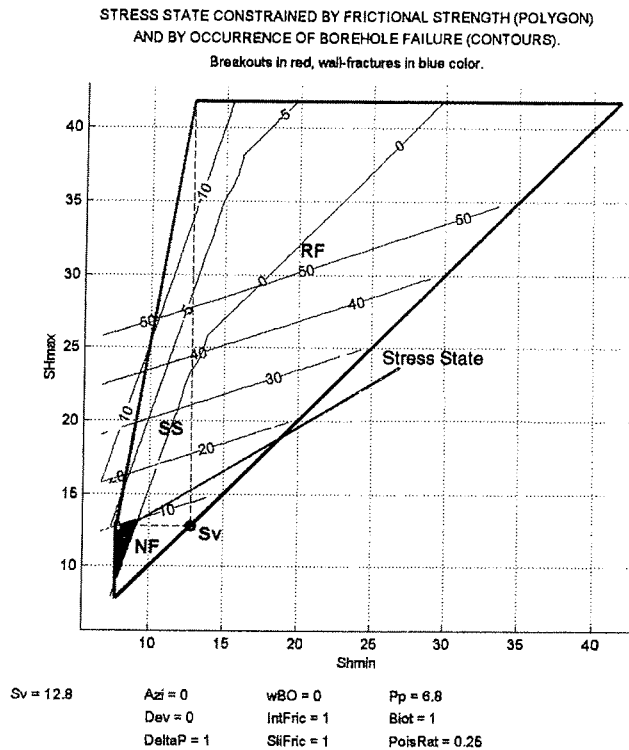


Fig. 9 - Stress analysis used to constrain horizontal stress magnitudes based on the presence of tensile failures and the absence of breakouts in the BHTV images from CRP-2.

## IMPLICATIONS

The Cape Roberts boreholes are sited within generally east-dipping depositional sequences immediately to the east of the Transantarctic Mountain front (Barrett et al., 1995; Hamilton et al., 1998). Dipmeter and seismic imaging results support the general trend of shallow eastward dips but indicate considerable variability at sub-seismic scales (Jarrard, et al.; Paulsen, et al; this volume). Orientations of clearly-defined stratigraphic horizons seen in the BHTV data confirm this general result, and also reveal a significant subset of sedimentary features generally found below 350 m with shallow west dips.

Natural fractures seen in BHTV images also have similar orientations to those detected in cores from this hole and CRP-1 (e.g., Wilson and Paulsen, 1999; Paulsen, et al., this volume), as these primarily dip steeply west and WSW with some east-dipping features, both previously identified by the above authors as normal faults. These features indicate a horizontal roughly ENE-WSW orientation of least principal stress at the time they were active, regardless of whether they formed initially as tensile features or are a consequence of normal faulting. The predominance of west-dipping features (nearly normal to stratigraphy) may indicate a tensile origin and their current orientation may be due to structural tilting associated with basin formation. More shallow-dipping features identified as fractures are either stratigraphic discontinuities or fractures initiated along weak bedding-parallel planes.

Drilling-induced failures clearly reveal that the current stress state is one of ENE-WSW extension, normal to the

orientation of the Transantarctic Mountains immediately west of the site. If the basin formed and continues to be active purely as an extensional feature, such a trend of ENE extension would be expected. Thus the stress orientation and low relative magnitudes of the horizontal stresses revealed from these data are consistent with pure normal faulting along the Transantarctic Mountains. While the stress orientation is well constrained, to further quantify stress magnitudes would require either laboratory rock strength measurements or collection of hydraulic fracturing stress measurements in this or future boreholes.

## ACKNOWLEDGEMENTS

This work was conducted with support of the first author by NSF Polar Research Program #OPP-9527412. We appreciate the constructive reviews and advice of David Goldberg. GeoMechanics International granted use of the GMI•Imager™ software with which the BHTV data were analyzed.

## REFERENCES

- Barrett P.J., Henrys S.A., Bartek L.R., Brancolini G., Busetti M., Davey F.J., Hannah M.J. & Pyne A.R., 1995. Geology of the margin of the Victoria Land basin off Cape Roberts, southwest Ross Sea. In: *Geology and Seismic Stratigraphy of the Antarctic Margin, Antarctic Research Series*, **68**, 183-207.
- Barton C.A., Tesler L. & Zoback M.D., 1991. Interactive analysis of borehole televiewer data. In: I.P.A.S. Sengupta (ed.), *Automated Pattern Analysis in Petroleum Exploration*, Chapter 12, Springer-Verlag, New York.
- Byerlee J. 1978. Friction of rocks, *Pure and Applied Geophysics*, **116**, 615-626.
- Cape Roberts Science Team, 1998. Initial Report on CRP-2, Cape Roberts Project, Antarctica. *Terra Antarctica*, **5**(1), 187 pp.
- Cape Roberts Science Team, 1999. Studies from the Cape Roberts Project, Ross Sea, Antarctica, Initial Report on CRP-2/2A. *Terra Antarctica*, **6**(1/2), 173 pp.
- Gough D.I. & J.S. Bell, 1981. Stress orientations from borehole wall fractures with examples from Colorado, east Texas, and northern Canada. *Can. J. Earth Sci.*, **19**, 1358.
- Hamilton R.J., Sorlien C.C., Luyendyk B.P., Bartek L.R. & Henrys S.A., 1998. Tectonic regimes and structural trends off Cape Roberts, Antarctica. In: Barrett P.J. & Ricci C.A. (eds.), *Studies from the Cape Roberts Project, Ross Sea, Antarctica - Scientific Report of CRP-1*, *Terra Antarctica*, **5**(3), 261-272.
- Kirsch G., 1898. Die Theorie der Elasticitaet und die Bedurfnisse der Festigkeitslehre", *VDI Z.*, **42**, 707.
- Li Y. & Schmitt D.R., 1997. Well-bore bottom stress concentration and induced core fractures, *AAPG Bulletin*, **81**(11), 1909-1925.
- Li Y. & Schmitt D.R., 1998. Drilling-induced core fractures and *in situ* stress, *J. Geophys. Res.*, **103**(3), 5225-5239.
- Lorenz J.C., Finley S.J. & Warpinski N.R., 1990. Significance of coring-induced fractures in Mesaverde core, northwestern Colorado, *Am. Assoc. Soc. Am. Bull.*, **74**, 1017-1029.
- Moos D. & M. D. Zoback, 1990. Utilization of observations related to wellbore failure to constrain the orientation and magnitude of crustal stresses: Application to continental, DSDP and ODP boreholes, *J. Geophys. Res.*, **95**, 9305.
- Wilson T.J., 1995. Cenozoic transtension along the Transantarctic Mountains - West Antarctic Rift boundary, Southern Victoria Land, Antarctica, *Tectonics*, **14**, 531-545.
- Wilson T.J. & Paulsen T.S., 1998. CRP-1 fracture arrays: constraints on the Neogene-Quaternary stress regime along the Transantarctic Mountains Front, Antarctica, In: Barrett P.J. & Ricci C.A. (eds.), *Studies from the Cape Roberts Project, Ross Sea, Antarctica - Scientific Report of CRP-1*, *Terra Antarctica*, **5**(3), 327-335.
- Zemanek J., Glenn E.E., Norton L.J. & Caldwell R.L., 1970. Formation evaluation by inspection with the borehole televiewer, *Geophysics*, **35**, 254-269.
- Zoback M. D. & J. H. Healy, 1984. Friction, faulting and in-situ stress, *Annales Geophysicae*, **2**, 689.
- Zoback M. D., D. Moos, L. Mastin & R. N. Anderson, 1985. Wellbore breakouts and in-situ stress, *J. Geophys. Res.*, **90**, 5523.
- Zoback M. L. et al., 1989. Global patterns of tectonic stress, *Nature*, **341**, 291.